JCRS

Journal of Chemical Reactivity and Synthesis 2023: 13(3) 177-201

Research Article

A Study on the Role of Nano silica Seeds on the Synthesis of Silica Colloids

Fatemeh Kholghi, Seyed Mojtaba Zebarjad*, Elham Katoueizadeh, Habib Daneshmanesh

Department of Materials Science and Engineering, School of Engineering, Shiraz University, Shiraz, Iran

ARTICLE INFO:

Received:

25 July 2023

Accepted:

14 August 2023

Available online:

16 September 2023

✉: M. Zebarjad

mojtabazebarjad@shirazu.ac.ir

ABSTRACT

In the current research sodium silicate has been used to synthesize silica colloid by ion exchange process. Deterministic relations for zeta potential, size and solid content have been developed by optimization of three input parameters: seed concentration (0, 1, 2%wt), temperature (30, 55, 80°C) and KOH concentration (0.5, 1, 1.5%wt). Central Composite Design of Response Surface Methodology was used to optimize silica colloid. The goal of this optimization is to achieve the silica colloid with the highest zeta potential, the minimum particle size and the highest solid content. The derived equations and contour plots predict the values of selected independent variables for preparation of optimum silica colloid with desired properties. Based on the fitted models, the optimum silica colloid is prepared by 0.756%wt KOH in 70°C that contains 59.9 %wt SiO_2. Also, this silica colloid sample contains a particle size of 11.5 nm and zeta potential of -6.48 mV.

Keywords: Nanosilica, Seed, Response surface methodology, Silicacolloids.

1. Introduction

Silica is increasingly attracting attention due to its extraordinary properties and potentials in wide variety technological applications. Silica colloids are composed of fine amorphous SiO_2 particles, usually spherical silica, dispersed in the liquid phase [1]. The specific surface area of nanocolloid silica is relatively large, which makes it more attractive in the environment applications [1]. They are a good idea for used as high temperature binder for inorganic paint, abrasive particles for mechanical polishing of silicon wafers [2], drainage aid in paper making [3] and abrasion resistant coatings [1], etc.

Silica colloid can be prepared by various methods including ion exchange [4], neutralization or electrodialysis of aqueous silicates, hydrolysis and condensation of silane [5], or milling of silica gel or powder [6] and direct oxidation of silicon to produce silica colloids [7]. In the current paper, it is tried to focus on the preparation of silica colloid from ion exchange method [8], which uses sodium silicate [1] as preferred raw material because of its low price and convenient availability, which also has the ability to produce silica colloids by ion exchange method, compared to the other alkali silicates that are available commercially such as silicon tetrachloride[9], tetraethoxysilane (TEOS) [10], sodium silicate [1] and silica powder [11]. Ion exchange is a simple, cheap and scale-up method used in industries [4]. Some researchers have used seeds in their experiments to prepare silica colloids. Coenen and De Kruif [12] used Stober process, but used commercial Ludox as the seeds to synthesized silica colloid particles. Coenen indicated that the particle size of composite silica (silica colloid is the core and silica from TEOS is the shell of this particle) can be estimated if assume the process under controlling in the surface control range. Chen [2] studied the new particle formation in the monosize silica seeds who used $Si(OH)_4$ from TEOS hydrolysis as the raw material. He indicated that the

new particles are formed in the certain conditions, such as the early stage of growth of silica particles are controlled by diffusion of condense species, and have electric charge against an electrostatic repulsion onto the surface of silica seeds. Several factors affect the properties of silica colloidal produced by ion exchange method. As a result, in order to obtain silica colloid with suitable properties such as high zeta potential, small particle size and high solid content, the factors affecting on the production process should be investigated. To have a successful test design, controllable variables must be identified and ultimate goals defined. When an answer is affected by several variables, it can be defined as a mathematical function of variables [13]. The response surface methodology (RSM) is a statistical tool in which there is a response that is affected by several variables and must be optimized [14]. In other words, to decrease the number of experiments and to conserve time it is necessary to perform RSM [15].

The RSM can determine the effect of the parameters individually as well as their interaction with each other on the results. Central composite design (CCD) is the most popular response surface methodology used for second-order models. In this study, CCD was used to design the experiment, which was suitable for complex surfaces. In this design, three sets of points including factorial, axial and central points are examined. The CCD method can be used for a maximum of 5 parameters. This method also provides an acceptable amount of non-compliance for testing. Also, this method does not require a large number of tests [13].

To the best of our knowledge, there are many articles concentrated on the production of nanosilica colloid [11,16,17]. But the role of seed concentration along with temperature and KOH concentration using RSM have not been under more attention. Therefore, in the current research it was tried to fill the literature gap in this issue.

In the previous research [18] , silica colloids were produced by ion exchange method using sodium silicate as the precursor. The effect of seed concentration, temperature and Potassium Hydroxide (KOH) concentration on zeta potential, solid content and particle size was studied using Response Surface Methodology (RSM). The stability of the solutions was evaluated by Zeta potential, Fourier-transform infrared spectroscopy (FTIR) and Dynamic Light Scattering analysis (DLS). The aim of this article was to model and optimize silica colloids using the RSM. The different operational parameters like seed concentration, temperature and KOH concentration were modeled through the CCD to forecast the output.

2. Materials and Method

a. Materials

Sodium silicate containing 7.5–8 %wt Na_2O and 25.5–28.5 %wt SiO_2 with 1.35 g/cm^3 density was used to prepare silica nanocolloids. Hydrochloric acid (HCl with density 1.2 g/cm^3 and 37% purity) was used for the reduction step. Potassium hydroxide (KOH with density 2.12 g/cm^3 and 98% purity) was also used. Also, nano silica particles with a particle size of less than 15nm in diameter from the company TECNAN, were used as a seed. Deionized (DI) water was used in all of the experiments.

b. Synthesis of silica nanocolloids

13 grams of sodium silicate was diluted with 40 ml of deionized water. Then, active silicic acid was produced by passing diluted sodium silicate through ion exchange resin. The sodium ions of the diluted sodium silicate solution were substituted by hydrogen ions on the exchange sites of cationic resin. The amount of initial solution pH after passing through the glass column decreases from 12 to about 2-3. Then, different concentrations of KOH solutions (0.5, 1, 1.5%wt) were prepared and heated to the desired temperatures (30, 55, 80°C). A solution that is heated to the desired temperature is called a heated solution.

To prepare some samples, the heated solution in addition to KOH, contained different concentrations of seeds (0, 1, 2%wt). Then active silicic acid was added to the heated solution while stiring at a constant rate of 0.5 ml/min. The experimental flow chart is shown in Figure 1. The stability of silica colloids is considered via accelerated aging test. By mixing with the cation exchange resin, potassium ions were removed and the pH value was reduced from 10 -11 to 2-3. The acidic slurry is placed in the oven at 65°C for 7 days. The solution is stable, if it doesnt turns to a gel state during the accelarated ageing test, otherwise, it shows an unstable behavior.

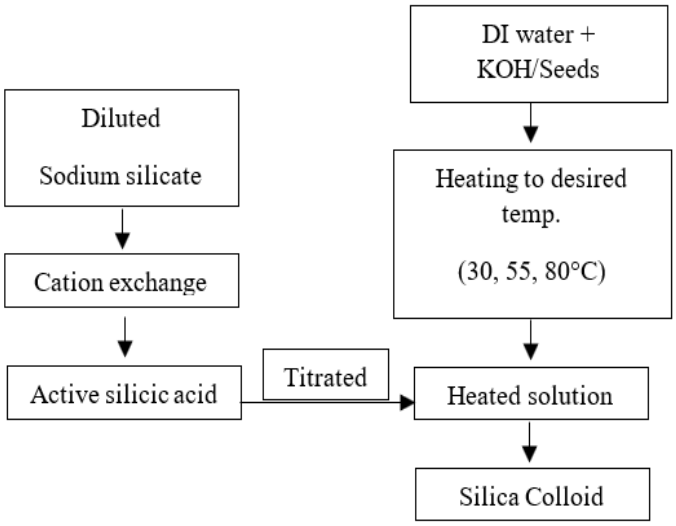

Figure 1: The experimental flowchart of formation colloidal silica.

c. Characterization

The quality of production samples will have a significant effect on the final properties of silica nanocolloid. In order to check the produced samples, different analyzes were performed, which are mentioned below. Zeta potential (model SZ-100) was used to determine the samples stability. In order to determine the chemical composition of the samples, Fourier-transform infrared spectroscopy (FTIR model Bruker Tensor II) was performed. Then, the prepared samples were optimised by RSM design. Dynamic Light Scattering analysis (DLS model SZ-100) was performed to determine particles size. Also to investigate the amount of

elements in the production samples, the X-ray fluorescence spectroscopy (XRF) test of S4PIONEER model from Bruker, Germany was performed. For this purpose, 40 ml of the sample was poured into a petri dish and placed in an oven at 120°C for 30 minutes. Then 1 g of the powder was collected for the above analysis. Then, in order to calculate the LOI, some of the sample was first weighed and then heated at 1000°C for two hours. Then weighed again. The difference between the two weights is reported as Loss on Ignition (LOI).

d. Experimental design

A central composite design was used as the experimental design to determine the relationship between the dependent variables (responses) and three independent variables (factors) over a specified region (Table 1). For the three factors, this design consisted of a full factorial design augmented by six axial points (or star points), with six replications of the center point, resulting in a total number of 20 experiments. The three selected factors for this experiment were the temperature, seed concentration and KOH concentration. Zeta potential, particle size, and solid content were measured as responses. The central composite design matrix showing the runs of experiment, factors and their levels is shown in Table 2: **Design matrix.**

Table 1: Design and parameter levels chosen

Variable	Unit	-1	0	+1
Temperature (A)	°C	30	55	80
KOH (B)	%wt	0.5	1	1.5
Seed (C)	%wt	0	1	2

Table 2: Design matrix

Run	**A** Temp (°C)	**B** KOH (%wt)	**C** Seed (%wt)
1	30	1.5	0
2	55	1	1
3	55	1	1

4	55	1.5	1
5	80	0.5	0
6	80	1	1
7	55	1	1
8	80	1.5	2
9	80	0.5	2
10	30	1	1
11	30	0.5	2
12	80	1.5	0
13	55	1	1
14	55	1	1
15	55	1	2
16	30	0.5	0
17	55	1	1
18	55	0.5	1
19	55	1	0
20	30	1.5	2

3. Results and Discussions

In order to optimize the synthesis parameters of silica nanocolloid, the results of the tests were analyzed by the surface response method in Design Expert software. The Table 3 shows the results in each test.

Table 3: Relevant results for the design of experiments using the response surface method

	Response 1	**Response 2**	**Response 3**
Run	zeta potential (mV)	Particle size (nm)	Solid Content (g/ml)
1	0.6	161.6	0.023
2	-3.6	203.8	0.076
3	-0.8	87.9	0.012
4	-4	161	0.106
5	-1.6	53.5	0.021

6	-11.2	78.5	0.044
7	-5.2	111.8	0.036
8	-6	123.2	0.13
9	-16.1	111.1	0.067
10	-10	324	0.061
11	-3.9	159.8	0.026
12	0.1	6.6	0.109
13	-1.9	161	0.026
14	-5	111.7	0.036
15	-8.1	87.4	0.011
16	-10.4	7.8	0.048
17	-7	111.3	0.092
18	-7.4	150.8	0.048
19	-8	14.2	0.071
20	15.3	142.9	0.017

a. Response Surface Methodology (RSM)

A coefficient of determination (R^2) determines the fit quality of the model and the F-value determines its statistical importance [19]. R^2 demonstrates the proportion of changes in response data that can be described by the fit model. Hence, the higher the R^2, the better the model. As shown in Table 4, the R^2 values for all responses / models are over 70%. It can be concluded that a supreme explanation of the relationship between the independent variables (factors) and the dependent variable (response) is provided by each regression model. The statistical importance of the proportion of mean squared changes because of regression and mean squared residual error was tested using analysis of variance (ANOVA). ANOVA is a statistical technique that distributes the total variability in a data collection into components related to particular change sources in order to examine the hypotheses on the model parameters [20]. ANOVA details of three responses are presented in Table 4**: ANOVA details of three responses.**

Table 4: ANOVA details of three responses

Source	Degree of freedom	Mean Square	F-value	P-value	Adequate precision	R-Squared (R^2)
Zeta potential	6	3.11	6.81	0.0019	13.3906	0.7586
Particle size	6	26.33	5.98	0.0035	8.6865	0.7340
Solid content	6	0.1706	12.26	0.0002	16.1000	0.8597

Degrees of Freedom is the number of estimated parameters used to compute the source's sum of squares. Mean Square (also called variance) is the sum of squares divided by the degrees of freedom. A p-value lower than 0.05 (or 95% confidence) represents that the model is considered to be statistically significant [21]. In Table 4**: ANOVA details of three responses**, the p-values for all of the regressions were lower than 0.05. This means that at least one of the terms in the regression equation has a significant relation with the response variable. Adequate precision is a signal to noise ratio. It compares the range of the predicted values at the design points to the average prediction error. Ratios greater than 4 show proportional model discrimination [21, 22]. As shown in Table 4**: ANOVA details of three responses**, all adequate precision of responses is above 4. In other words, the form of the model chosen to explain the relationship between the factors and the response is correct.

b. Zeta Potential

Zeta potential is measured and the obtained response surfaces are plotted as 3D surface plot in Figure 2. As shown in Figures (2a to 2c), at different concentrations of seed, zeta potential become more positive with increasing temperature or KOH concentration. In addition, in different concentration of KOH (shown in Figures 2d to 2f), zeta potential become more positive with increasing temperature or seed concentration. However, at different temperatures (Figure 2g to 2k), zeta potential become more positive with

increasing KOH concentration and more negative with increasing seed concentration. The calculated coded equation for zeta potential is presented in Equation 1, where A, B and C represent temperature, KOH and seed concentration, respectively. According to the graphs obtained from the zeta potential model, it can be shown that KOH concentration has the greatest effect on zeta potential changes.

$$(Zeta\ potential\ +\ 17.71)^{0.56} = (-0.4831)A + (0.8358)B + (-0.1211)C + (-0.2312)AB + (-0.9728)AC + (0.3844)BC + 4.09 \quad \text{Eq. (1)}$$

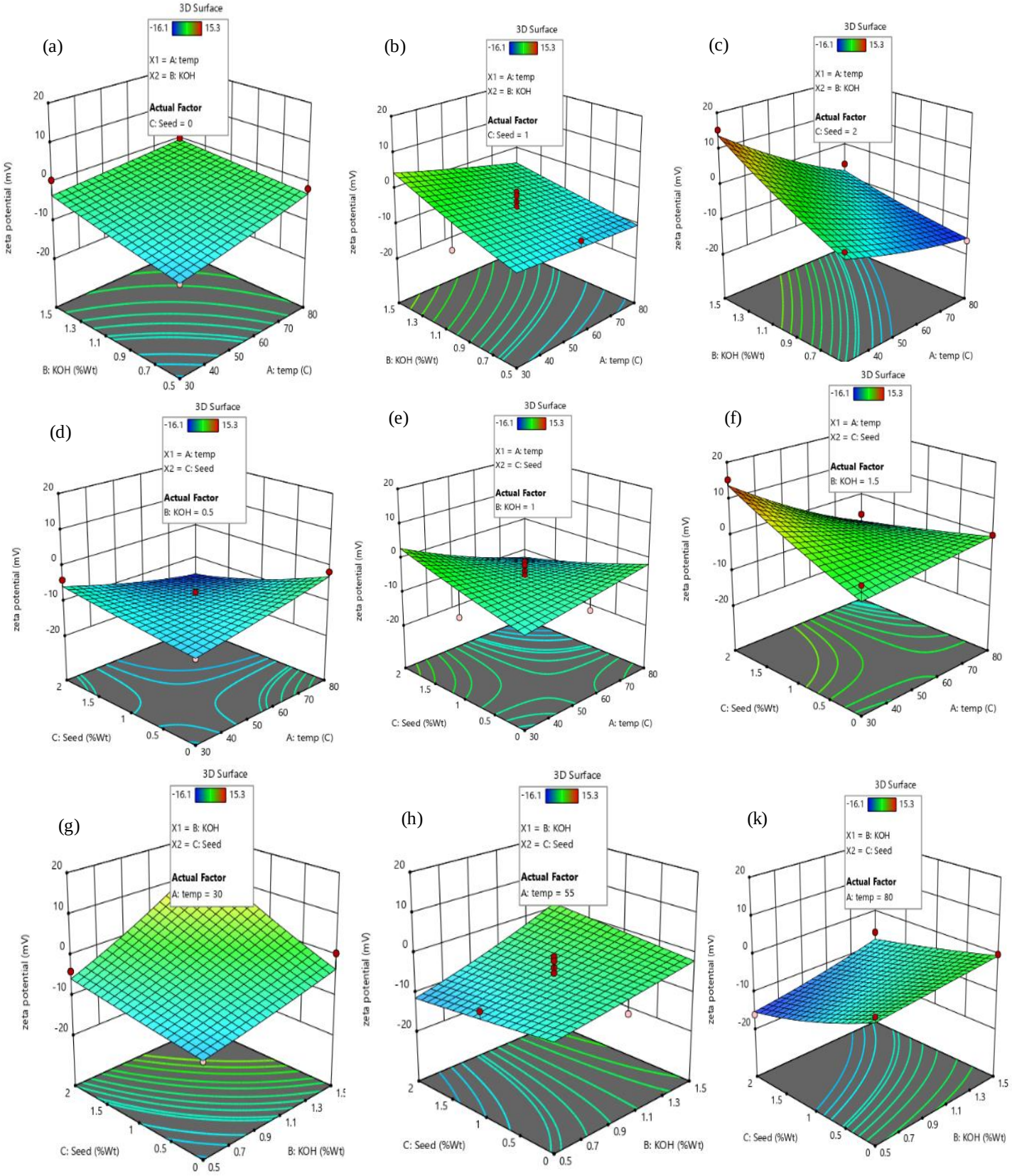

Figure 2: 3D surface plot of the impact of: (a-c) temp. and KOH at constant seed, (d-f) temp. and seed at constant KOH, (g-k) KOH and seed at constant temp on zeta potential

According to the 3D surface plot of zeta potential, it can be seen that at constant one parameter and increasing the other two parameters, the zeta potential improves. The main reason of this variation can be attributed to the fact as the temperature increases, the kinetic energy of the particles increases resulting the surface adsorption decreases. Also, the electric double layer becomes less compressed and the ionic strength decreases [23]. Also, with increasing KOH concentration, the solution becomes more alkaline and the particles tend to acquire more negative charge, and as a result, the zeta potential goes to more negative numbers [24]. According to what proposed by Lee [25], the mobility of nano colloidal particles decreased as salt concentration increased. Eq. (2) shows the relationship between mobility of nano colloidal particles and zeta potential, where μ_E is the electrophoretic mobility, ε; dielectric constant, ζ; zeta potential, κ ; the reciprocal electrical double layer which depends on ionic strength of the solution, a; the radius of the biomolecules, f (κa); Henry's corrective term and η is the viscosity of solution. It can be said that an increase in salt concentration, causes to decreases the nano colloid particles mobility and subsequently the zeta potential decreases [26].

$$\mu_E = (2\varepsilon\zeta f(\kappa a))/(3\eta) \quad \text{Eq. (2)}$$

c. Particle Size

Response surface model of particle size is shown in Figure 3. The results indicate that the particle size increases by decreasing the temperature or increasing the concentration of KOH (Figure 3a to 3c). However, in different concentration of KOH, particle size increases with decreasing temperature or increasing seed concentration up to 1.25%wt (Figure 3d to 3f). also in different temperature, particle size increases with increasing KOH concentration or increasing seed concentration up to 1.25%wt (Figure 3g to 3k). The coded equation for particle size is according to Eq. (3). According to the graphs obtained

from the particle size model, it can be shown that seed concentration has the greatest effect on particle size changes.

$$(Size)^{0.48} = (1.82)A^2 + (-4.19)C^2 + (-1.54)A + (0.4767)B + (2.35)C + (-1.50)AB + 10.48$$

Eq. (3)

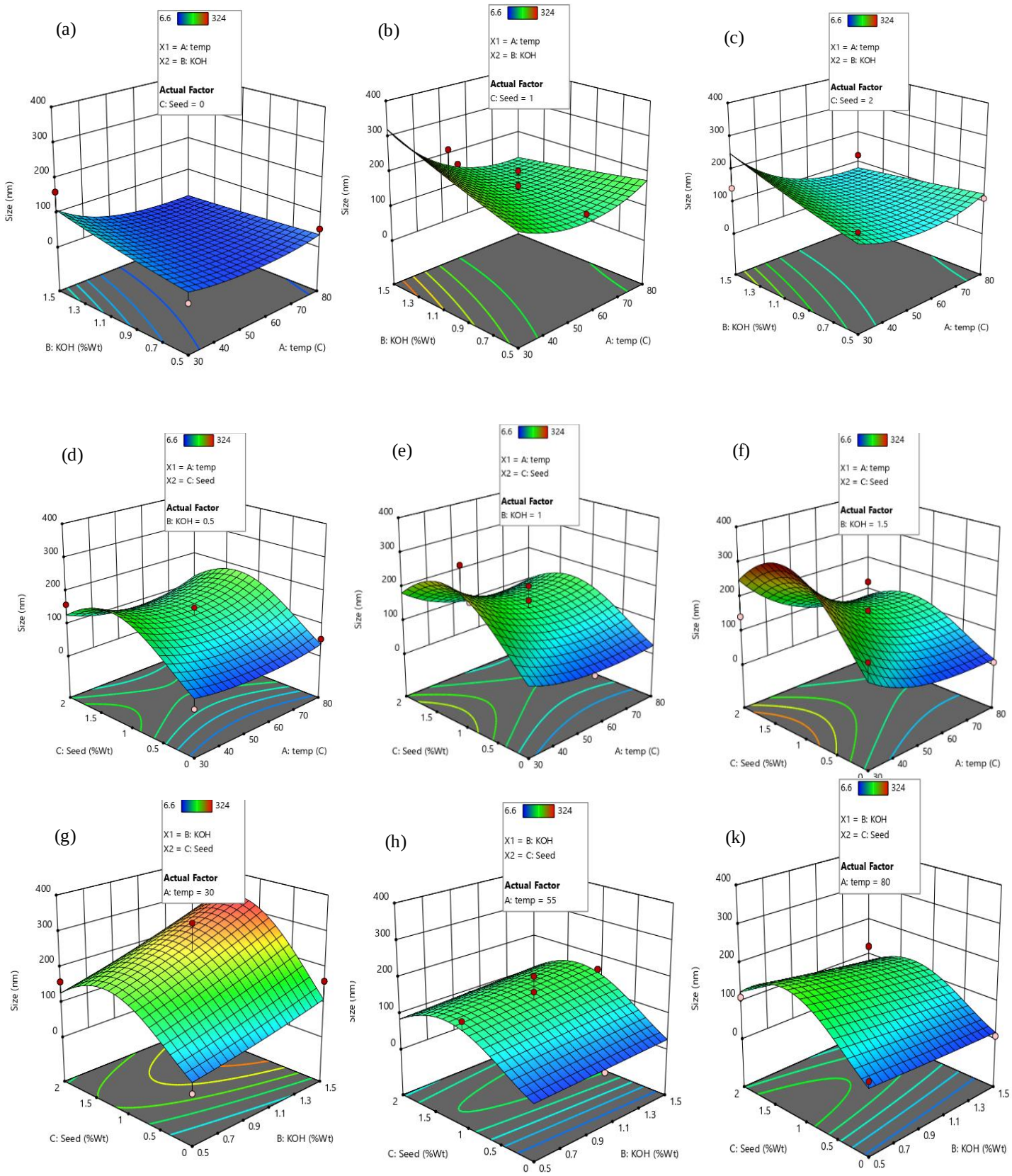

Figure 3: 3D surface plot of the impact of: (a-c) temp. and KOH at constant seed, (d-f) temp. and seed at constant KOH, (g-k) KOH and seed at constant temp on particle size

According to the 3D surface plot related to the particle size, it can be seen that in constant seed concentration, increasing temperature and decreasing KOH percentage, it has a positive effect on particle size. Also, at a constant %wt KOH, the size of the soluble particles decreases with increasing temperature and decreasing seed percentage. At constant temperature, the particle size of the solute increases with increasing seed and KOH percentage. It should be noted that the smaller the particle size of the solution, the more desirable it is. Under seed conditions, silica colloidal particles tend to form on the surface of seed particles, which increases the particle size. Eq. (4) shows the relationship between solution concentration and ionic strength [27]. In this relation, Ionic strength (I), is a measure of the concentration of electrically charged species in solution, c_i^{∞} is the concentration of the solution and z is the ion capacity of the solution. For solutions of relatively low ionic strength, ion surrounded by an atmosphere of ions of the same charge, but which is opposite to that of the central ion. The ionic atmosphere lowers the chemical potential of the central ion by neutralizing its charge. If A and B have charges of the same sign, a high ionic strength favors the formation of encounter pairs having a higher charge and, consequently, increases the rate of reaction. The increase in I increases the rate constant for reactions between ions of the same charge and decreases it when the ions are oppositely charged [27]. According to this relationship, it can be shown that with increasing the concentration of the solution, the ionic strength increases. Also, the relationship between the thickness of the electric double layer for the aqueous solution and the ionic strength is given in Eq. (5) In this relation, $\frac{1}{k}$ is the thickness of the electric double layer and I is the ionic strength [26]. As, the KOH concentration increases, the electrical conductivity of the solution increases, compressing the thickness of the double electrical layer of the silica colloid. This simplifies the particle growth process and increases the particle size [17].

$$I = \frac{1}{2} \times \sum_i c_i^{\infty} \times z_i^2 \qquad \text{Eq. (4)}$$

$$\frac{1}{k} = (1.8 \times 10^{16} \times I)^{-0.5}$$ Eq. (5)

d. Solid Content

Figure 4 show response surface model of solid content. As shown in the plots, in different concentration of seed, solid content increases with increasing temperature or decreasing KOH concentration (Figure 4a to 4c). However, in different concentration of KOH, solid content increases with increasing temperature or decreasing seed concentration (Figure 4d to 4f). Also in different temperature, solid content decreases with increasing KOH concentration or increasing seed concentration (Figure 4g to 4k). The coded equation for solid content is according to Eq. (6) Terms A, B and C represent temperature, KOH and seed concentration, respectively. According to the graphs obtained from the solid content model, it can be shown that seed concentration has the greatest effect on solid content changes.

$$(Solid\ content)^{2.32} = (0.1498)A + (-0.1441)B + (0.1059)C + (0.0733)AB + (0.2474)BC + (-0.1782)AC + 0.9597$$ Eq. (6)

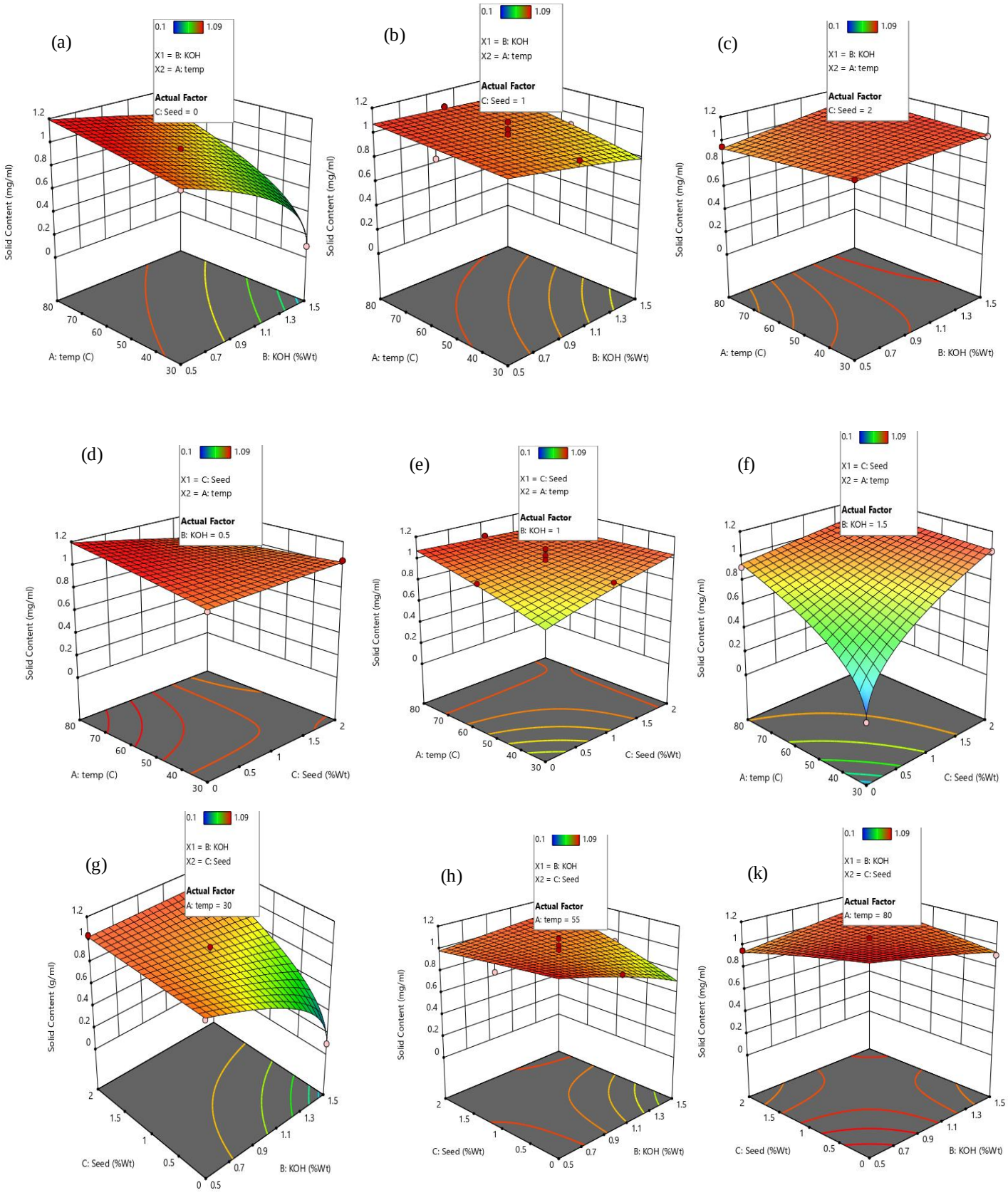

Figure 4: 3D surface plot of the impact of: (a-c) temp. and KOH at constant seed, (d-f) temp. and seed at constant KOH, (g-k) KOH and seed at constant temp. on solid content

e. Optimization by RSM

In order to determine the optimal sample, the range of changes of all three factors was selected in the range. The target was also set for the zeta potential and the solid content maximum value and for the particle size minimum value. Optimization of the synthesis parameters was carried out by the application of RSM, in order to maximize the zeta potential and the solid content and to minimize the particle size. Two samples, 1 and 2 were chosen. Also, to better understand the effect of seed concentration on the properties of the silica colloid, select one sample with and one without seed. Table 5 shows the experiments suggested by the Design expert software. According to results, as the temperature increases, the kinetic energy of the particles increases and as a result the adsorption decreases and the electric double layer becomes less compressed and the ionic strength decreases and as a result the zeta potential goes towards more positive numbers [23]. As it is known, with increasing ionic strength, the electric double layer becomes thinner and thus the zeta potential decreases [28].

Table 5: Selected examples from software suggested

Num.	Temp. (°C)	KOH (% wt)	Seed (% wt)	Zeta potential (mV)	Particle size (nm)	Solid content (g/ml)
1	80.000	0.979	0.045	-7.63	9.7	0.012
2	70.100	0.756	0.000	-6.48	11.5	0.050

Table 6 shows the values predicted by the RSM and the actual values obtained from the repetition of these two tests. As a result, it can be shown that the appropriate optimization has been selected and the resulting values are more desirable than the predicted values. Also, the selected models are desirable for all three responses. After that, sample 2 was selected as the optimal sample. Due to its lower operating temperature (70°C) than the sample 2 (80°C). Also, seeds were not used in the preparation of sample 2, which in itself can contribute to greater stability of the solution.

Table 6: measurement results for 1 and 2 samples

	Particle size (nm)		Zeta potential (mV)		Solid content (g/ml)	
Num.	**Predicted**	**Obtained**	**Predicted**	**Obtained**	**Predicted**	**Obtained**
1	25.536	9.7	-2.3	-7.63	0.012	0.023
2	16.837	11.5	-5.288	-6.48	0.050	0.053

f. Fourier-transform infrared spectroscopy (FTIR)

In order to investigate the chemical composition of the sample 2, FTIR test was performed, which is shown in Figure *5*. The three peaks assigned to the different vibration modes of the Si-O-Si group are distinguished. They are classified according to the nature of the motion of the ratio atom, due to its low mass to the silicon atom. First, the 1080 cm^{-1} peak, which is the main and most intense, represents the net tensile vibration of the Si-O-Si bonds. This vibration is due to the displacement in the plane defined by Si-O-Si parallel to the Si-Si axis. Second, the peak at 800 cm^{-1} is dedicated to the vibration of Si-O-Si bonds. The atom of the device on the Si–O–Si plane moves in the bisector of the Si–O–Si angle. Finally, the peak at 460 cm^{-1} is attributed to the bending vibration of Si-O-Si bonds. The atom leaves the Si–O–Si plane. In addition, the peak at 960 cm^{-1} is assigned to a stretching vibration of Si–OH bonds [29].

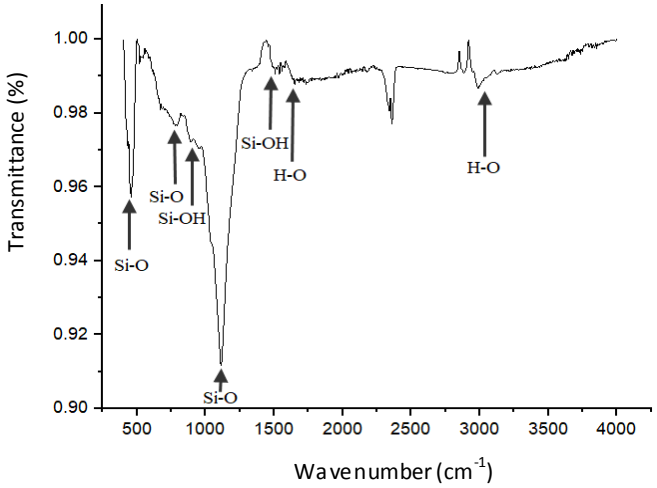

Figure 5: FTIR test of sample 2

g. X-ray fluorescence spectroscopy (XRF)

In order to determine the SiO_2 percentage in the optimal sample, a XRF test was performed. The results (Table 7) show that the sample contains a 59.9 %wt SiO_2 that is a significant percentage. It should be noted that the variation of the concentration of silica in the silica colloid sample produced by the ion exchange method reported by other researchers [1,30] is range of 18.8-25 %wt.

Table 7: XRF result of sample 2

Composition of sample 2	percentage (%w/w)
SiO_2	59.90
K_2O	29.10
P_2O_5	0.820
CaO	0.530
Cl	0.380
SO_3	0.190
Al_2O_3	0.180
Na_2O	0.160
Fe_2O_3	0.100
CuO	0.079
LOI	8.54
Total	99.98

4. Conclusions

In the current research of synthesized silica was investigated. For this purpose, some different parameters such as seed concentration (0, 1, 2 %wt), temperature (30, 55, 80°C) and KOH concentration (0.5, 1, 1.5 %wt) was changed and to optimized the three significant parameters, RSM employed. The results of current research are remark as follow: The results of zeta potentials show that at constant one parameter and increasing the other two parameters, the zeta potential improves and KOH concentration has the greatest effect on zeta potential changes. Also, the result of particle size show that in

constant seed concentration, increasing temperature and decreasing KOH percentage, it has a positive effect on particle size. At a constant concentration KOH, the size of the soluble particles decreases with increasing temperature and decreasing seed percentage. At constant temperature, the particle size of the solute increases with increasing seed and KOH percentage and seed concentration has the greatest effect on particle size changes. The result of solid content show that in different concentration of seed, solid content increases with increasing temperature or decreasing KOH concentration. However, in different concentration of KOH, solid content increases with increasing temp or decreasing seed concentration. Also in different temperature, solid content decreases with increasing KOH concentration or increasing seed concentration and seed concentration has the greatest effect on solid content changes. Based on the fitted models, the optimum silica colloid sample is prepared by 0.756%wt KOH in 70°C condition that contains 59.9 %wt SiO_2. In addition, this silica colloid sample contains a particle size of 11.5 nm and zeta potential of -6.48 mV.

References

[1] S. Hassani, A. Rashidi, M. Adinehnia, N. Montakhaba, Facile and economic method for preparation of nano-colloidal silica with controlled size and stability, J. Nano dimension 5 (2013) 177-185. https://dorl.net/dor/20.1001.1.20088868.2014.5.2.11.9.

[2] P. L. Chen, J. H. Chen, M. S. Tsai, B. T. Dai, Post-Cu CMP cleaning for colloidal silica abrasive removal, J. Microelectronic engineering 75 (2004) 352–360. https://doi.org/10.1016/j.mee.2004.06.006.

[3] Y. J. Kang, Y. N. Prasad, I. K. Kim, S. J. Jung, J. G. Park, Synthesis of Fe metal precipitated colloidal silica and its application to W chemical mechanical polishing (CMP) slurry, J. Colloid interface science 349 (2010) 402-407.

https://doi.org/10.1016/j.jcis.2010.04.083.

[4] A. Yoshida, Silica nucleation, polymerization, and growth preparation of monodispersed sols, J. Colloid chemistry of silica 234 (1994) 51-66. DOI: 10.1021/ba-1994-0234.ch002

[5] W. Stober, A. Fink, Controlled growth of monodisperse silica spheres in the micron size range, J. Colloid and interface science 26 (1968) 62- 69. https://doi.org/10.1016/0021-9797(68)90272-5.

[6] Y. K. Lee, Y. R. Yoon, H. K. Rhee, Preparation of colloidal silica using peptization method, J. Colloids and surfaces A: Physicochemical and engineering aspects 173 (2000), 109-116. https://doi.org/10.1016/S0927-7757(00)00601-4.

[7] H. Lima, W. K. Na, H. M. Lim, S, H. Huh, S. E. Park, Y. S. Lee, S. H. Lee, Effect of the average particle size and the surface oxidation layer of silicon on the colloidal silica particle through direct oxidation, J. Materials Science and Engineering B 163 (2009) 82–87. https://doi.org/10.1016/j.mseb.2009.05.011.

[8] M. S. Tsai, The study of formation colloidal silica via sodium silicate, J. Materials science and engineering B 106 (2004) 52–55. https://doi.org/10.1016/j.mseb.2003.08.052.

[9] Z. R. Luo, Y. Hong, L. S. Wang, W. G. Feng, Preparation of silica nanoparticles using silicon tetrachloride for reinforcement of PU, J. Chemical engineering 187 (2012) 357–366. https://doi.org/10.1016/j.cej.2012.01.098.

[10] K. Tadanaga, K. Morita, K. Mori, M. Tatsumisago, Synthesis of monodispersed silica nanoparticles with high concentration by the Stöber process, J. Sol-Gel Science and Technology 68 (2013) 341–345. https://doi.org/10.1007/s10971-013-3175-6.

[11] H. Mi Lim, J. Lee, J. H. Jeong, S. G. Oh, S. H. Lee, Comparative study of various preparation methods of colloidal silica, J. Engineering 2 (2010) 998–1005. http://dx.doi.org/10.4236/eng.2010.212126.

[12] S. Coenen, C. G. DE kruif, Synthesis and growth of colloidal silica particles, J. Colloid and interface science 124 (1987) 104- 108. https://doi.org/10.1016/0021-9797(88)90330-X.

[13] D. C. Montgomery, Design and analysis of experiments, ten ed., John wiley & sons, 2017.

[14] S. Beg, M. Rahman, A. Jain, S. Saini, P. Midoux, C. Pichon, F. J. Ahmad, S. Akhtar, Nanoporous metal organic frameworks as hybrid polymer–metal composites for drug delivery and biomedical applications, J. Drug discovery today 22 (2017) 625–637. https://doi.org/10.1016/j.drudis.2016.10.001.

[15] S. Ahmadi, M. Mesbah, C. A. Igwegbe, C. D. Ezeliora, C. Osagie, N. A. Khan, G. L. Dotto, M. Salari, M. H. Dehghani, Sono electro-chemical synthesis of LaFeO3 nanoparticles for the removal of fluoride: Optimization and modeling using RSM, ANN and GA tools, J. Environmental Chemical Engineering 9 (2021). https://doi.org/10.1016/j.jece.2021.105320.

[16] M. S. Tsai, P. Y. Huang, C. H. Yang, Formation mechanisms of colloidal silica via sodium silicate, J. Nanoparticle Research 8 (2006) 943–949. https://doi.org/10.1007/s11051-005-9047-4.

[17] M. S. Tsai, P. Y. Huang, W. C. Wu, The study of formation process of colloidal silica, J. Materials Research Bulletin 40 (2005) 1609–1616. https://doi.org/10.1016/j.materresbull.2005.04.035.

[18] F. Kholghi, E. Katoueizadeh, M. Zebarjad, H. Daneshmanesh, Investigating the Effect of Temperature on the Formation of Silica Nanocolloids Synthesized by Ion Exchange Method, UFGNSM 2021 Conference. Tehran, Iran (2021).

[19] S. J. M. Breig, K. J. K. Luti, Response surface methodology: A review on its applications and challenges in microbial cultures, J. Materials Today: Proceedings 42 (2021) 2277–2284. https://doi.org/10.1016/j.matpr.2020.12.316.

[20] Z. Li, D. Lu, X. Gao, Optimization of mixture proportions by statistical experimental design using response surface method - A review, J. Building Engineering 36 (2021) 1-44. https://doi.org/10.1016/j.jobe.2020.102101.

[21] C. A. Igwegbe, L. Mohmmadi, S. Ahmadi, A. Rahdar, D. Khadkhodaiy, R. Dehghani, S. Rahdar, Modeling of adsorption of Methylene Blue dye on Ho-CaWO4 nanoparticles using Response Surface Methodology (RSM) and Artificial Neural Network (ANN) techniques, J. MethodsX 6 (2019) 1779–1797. https://doi.org/10.1016/j.mex.2019.07.016.

[22] J. Rajewski, A. D. Inger, Application of response surface methodology (Rsm) for the optimization of chromium(iii) synergistic extraction by supported liquid membrane, J. Membranes (Basel) 11 (2021) 1-17. https://doi.org/10.3390/membranes11110854.

[23] A. Karami, Gh. R. Vahdani, M. Abedi, M. Fatahi, Preparation and characterization of colloidal silica in alkaline and constant range of pH, J.Chemistry chemical engineering 27 (2008) 65-70.

[24] J. Lyklema, Fundamentals of interface and colloid science: soft colloids, first ed., Elsevier Academic Press, 2005.

[25] H. M. Lee, Y. W. Kim, J. K. Baird, Electrophoretic mobility and zeta-potential of lysozyme crystals in aqueous solutions of some 1 : 1 electrolytes, J. Crystal growth 232 (2001) 294-300. https://doi.org/10.1016/S0022-0248(01)01071-5.

[26] S. Salgın, U. Salgın, S. Bahadır, Zeta Potentials and Isoelectric Points of Biomolecules: The Effects of Ion Types and Ionic Strengths, J. Electrochemical Science 7 (2012) 12404 – 12414.

[27] L. Arnaut, S. Formosinho, H. Burrows, Chemical kinetics _ from molecular structure to chemical reactivity, second ed., Elsevier Inc, 2021.

[28] E. Lee, Electrophoretic Motion of a Rigid Spherical Particle Normal to a Solid Plane, J. Interface Science and Technology 26 (2019) 65-85. https://doi.org/10.1016/B978-0-08-100865-2.00003-5.

[29] A. Chaouachi, R. Chtourou, A. M'nif, A. H. Hamzaoui, Optical characterization of colloidal silica crystals with controlled size microspheres, J. Materials Letters 116 (2014) 420–424. https://doi.org/10.1016/j.matlet.2013.11.069.

[30] N. Montakhab, H. Arabi, M. R. Aboutalebi, M. Alizadeh, S. S. Hassani, Control of Particle Size and Concentration of Colloidal Silica Formed via Cation Exchange Resin by Water Glass Solution, (2013) 25-38.